J|A|C|S
ARTICLES

Published on Web 07/24/2009

Measurement of Methyl Axis Orientations in Invisible, Excited States of Proteins by Relaxation Dispersion NMR Spectroscopy

Andrew J. Baldwin, D. Flemming Hansen, Pramodh Vallurupalli, and Lewis E. Kay*

Departments of Molecular Genetics, Biochemistry and Chemistry, The University of Toronto, Toronto, Ontario, Canada M5S 1A8

Received May 13, 2009; E-mail: kay@pound.med.utoronto.ca

Abstract: Few detailed studies of transiently populated conformations of biological molecules have emerged despite the fact that such states are often important to processes such as protein folding, enzyme catalysis, molecular recognition and binding. A major limitation has been the lack of experimental tools to study these often invisible, short-lived conformers. Recent advances in relaxation dispersion NMR spectroscopy are changing this paradigm with the potential to generate high resolution structural information which is necessary for a rigorous characterization of these states. In this study, we present an experimental method for establishing the relative orientations of methyl groups in invisible, excited states of proteins by measuring methyl $^{1}H-^{13}C$ residual dipolar couplings (RDCs). In our approach, four two-dimensional spectra are acquired at a pair of static magnetic fields. Each spectrum contains one of the four isolated multiplet components of a coupled methyl carbon, whose signal intensities, modulated by the pulsing frequency of a Carr−Purcell−Meiboom−Gill (CPMG) element, are sensitive to both chemical shift and RDC differences between exchanging states. In addition, data sets from a CPMG experiment which monitors the decay of in-phase methyl ^{13}C magnetization are recorded, that are sensitive only to the differences in chemical shifts between the states. Using our methodology, RDC values obtained from an invisible state in an exchanging system are shown to be in good agreement with the corresponding values measured under conditions where the invisible state is stabilized to become the highly populated ground state. The approach allows the measurement of anisotropic restraints at methyl positions in excited states and complements previously developed experiments focusing on the protein backbone.

Introduction

The function of biological molecules is often predicated on their interconversion between highly populated, ground-state conformations and low populated, transiently formed 'excited states'.[1−3] Ground-state conformers can often be characterized in detail using biophysical tools that include X-ray diffraction, nuclear magnetic resonance (NMR) spectroscopy and, increasingly, electron microscopy. In contrast, the low population and short lifetimes of many excited states complicate their study using traditional tools of structural biology. Detailed information about such excited states can be obtained, however, using CPMG relaxation dispersion NMR spectroscopy[4,5] in which relaxation rates of transverse magnetization derived from NMR active probes of the ground state are measured as a function of the rate of application of refocusing pulses which attenuate the effects of the exchange process. The relaxation rates are interpreted in terms of a model of exchange from which the kinetics and thermodynamics of the process are obtained as well as the chemical shifts of the often invisible excited state.[6−8] This information can be extracted so long as the interconversion rate between excited- and ground-state conformers is on the order of a hundred to a few thousand per second and the population of the excited state is above approximately 0.5%.

For many years the chemical shifts of backbone resonances of the ground states of proteins have been used in structural studies by converting them into dihedral angle restraints that complement measures of distances provided by NOEs.[9] More recently such chemical shifts have been used as the exclusive experimental restraints in concert with database protocols to generate high-quality backbone conformations of small to moderately sized proteins.[10,11] It is clear that the measurement of accurate chemical shifts of spin-probes in the excited state is critical for structural studies of these elusive conformers. In

(1) Karplus, M.; Kuriyan, J. *Proc. Natl. Acad. Sci. U.S.A.* **2005**, *102*, 6679–6685.
(2) Henzler-Wildman, K. A.; Lei, M.; Thai, V.; Kerns, S. J.; Karplus, M.; Kern, D. *Nature* **2007**, *450*, 913–916.
(3) Boehr, D. D.; McElheny, D.; Dyson, H. J.; Wright, P. E. *Science* **2006**, *313*, 1638–1642.
(4) Carr, H. Y.; Purcell, E. M. *Phys. Rev.* **1954**, *54*, 630–638.
(5) Meiboom, S.; Gill, D. *Rev. Sci. Instrum.* **1958**, *29*, 688–691.
(6) Palmer, A. G.; Kroenke, C. D.; Loria, J. P. *Methods Enzymol.* **2001**, *339*, 204–238.
(7) Palmer, A. G.; Grey, M. J.; Wang, C. *Methods Enzymol.* **2005**, *394*, 430–465.
(8) Korzhnev, D. M.; Salvatella, X.; Vendruscolo, M.; Di Nardo, A. A.; Davidson, A. R.; Dobson, C. M.; Kay, L. E. *Nature* **2004**, *430*, 586–590.
(9) Cornilescu, G.; Delaglio, F.; Bax, A. *J. Biomol. NMR* **1999**, *13*, 289–302.
(10) Cavalli, A.; Salvatella, X.; Dobson, C. M.; Vendruscolo, M. *Proc. Natl. Acad. Sci. U.S.A.* **2007**, *104*, 9615–9620.
(11) Shen, Y.; et al. *Proc. Natl. Acad. Sci. U.S.A.* **2008**, *105*, 4685–4690.

10.1021/ja903896p CCC: $40.75

this regard a large number of CPMG-based experiments and the appropriate isotopic labeling protocols have been designed for applications involving proteins that enable the measurement of excited state chemical shifts of main-chain ^{15}N, ^{1}HN, $^{1}H^{\alpha}$, $^{13}C^{\alpha}$ and ^{13}CO probes[12−17] as well as side-chain $^{13}C^{\beta}$ spins[18] and methyl groups.[19,20]

In addition to the measurement of a variety of different chemical shifts of backbone and side-chain probes in the exited state it has recently become possible to obtain RDCs and residual chemical shift anisotropies (RCSAs) when variants of the CPMG relaxation dispersion experiments are applied to molecules dissolved in solutions that promote weak alignment.[21−23] Spin-state selective relaxation dispersion experiments have been developed in which differences in RDCs between ground- and excited-state conformers are measured, and anisotropic restraints in the form of main-chain $^{1}HN-^{15}N$, $^{1}H^{\alpha}$-$^{13}C^{\alpha}$, $^{1}HN-^{13}CO$ RDCs have been reported in protein studies, in addition to experiments that determine the change in ^{13}CO chemical shifts upon alignment.[21,23,24] In an application involving an invisible, low populated state of an SH3 domain it has recently been shown that the combination of chemical shifts and anisotropic restraints obtained exclusively from CPMG studies was sufficient to produce a high resolution backbone fold of this conformer.[25]

Despite the initial success with studies of protein excited states that are based exclusively on backbone restraints, it would clearly be of interest to extend the methodology to probes along the side chain. An obvious first place to start is with methyl groups that are sensitive indicators of structure and dynamics in protein molecules.[26,27] A variety of robust methods for measuring methyl $^{1}H-^{13}C$ RDCs in ground state, highly populated conformations of proteins is available.[28,29] A study of chemical exchange using methyl $^{1}H-^{13}C$ RDCs has also recently emerged where differences in residual dipolar couplings were measured using CPMG-based ^{13}C direct observe spectroscopy of an aligned sample of a small molecule.[22] Here we build upon this work by presenting a spin-state selective two-dimensional CPMG experiment for measuring excited-state methyl $^{1}H-^{13}C$ RDCs in protein samples. The methodology is applied to a protein, ligand-binding system for which extensive cross-validation is possible, and it is established that accurate excited-state RDC values are obtained. The experiment thus promises to extend CPMG relaxation dispersion studies of excited protein states to include descriptions of structure and dynamics of methyl-containing side-chains.

Materials and Methods

Sample Preparation. ^{15}N-, ^{2}H-, Ile-[$^{13}CH_3$-δ1]-, Leu-, Val-[$^{13}CH_3$,$^{12}CD_3$]-labeled Abp1p SH3 domain[30−32] was prepared by protein overexpression in *Escherichia coli.* (BL21(DE3)) grown in D_2O and M9 media with ^{12}C,^{2}H glucose and ^{15}N ammonium chloride as carbon and nitrogen sources, respectively, and with the precursors α-ketobutyrate [$^{13}CH_3CD_2COCO_2Na$] and α-isovalerate [$^{13}CH_3(CD_3)CDCOCO_2Na$] added one hour prior to induction of protein overexpression to obtain the appropriately labeled methyl groups.[33,34] Details of protein expression and purification have been presented elsewhere.[21] The final protein concentration was ∼1.5 mM, in a buffer consisting of 50 mM sodium phosphate, 100 mM NaCl, 1 mM EDTA, 1 mM NaN_3, 100% D_2O, pH = 7 (uncorrected). ^{2}H Ark1p peptide,[35] which binds the SH3 domain, was expressed and purified as described previously.[21] Nine mole percent peptide was added to the Abp1p sample, verified by ^{13}C CW relaxation dispersion experiments that quantify the fraction of bound protein (Figure 1). Sample alignment was achieved through the addition of approximately 50 mg/mL Pf1 phage[36] (ASLA Biotech) giving rise to a D_2O splitting of 57 Hz at 25 °C and methyl $^{1}H-^{13}C$ RDCs of the apo-state of the protein in the range ±9.5 Hz. A second sample of 200 μM fully bound (holo) Abp1p SH3 domain was prepared for measurements of chemical shifts, $^{1}H-^{13}C$ scalar and dipolar couplings of the bound conformer to be used for cross validation. In this case approximately 40 mg/mL Pf1 phage was used, corresponding to a 46 Hz D_2O splitting (25 °C), with methyl RDCs of the bound form in the range ± 20 Hz.

NMR Spectroscopy and Data Analysis. A set of 20 constant-time CPMG relaxation dispersion data sets were recorded with the schemes of Figure 1, T_{relax} = 40 ms, using a fractionally aligned sample of Abp1p SH3/9% Ark1p peptide, at 25 and 5 °C, with 19 CPMG frequencies between 25 and 1000 Hz for each dispersion curve along with 1 reference ($N = 0$). Data sets were obtained at a pair of static magnetic field strengths corresponding to ^{1}H resonance frequencies of 500 and 800 MHz, with each spectrometer equipped with a room temperature probe. Spin-state selective data

(12) Loria, J. P.; Rance, M.; Palmer, A. G. *J. Am. Chem. Soc.* **1999**, *121*, 2331–2332.
(13) Tollinger, M.; Skrynnikov, N. R.; Mulder, F. A. A.; Forman-Kay, J. D.; Kay, L. E. *J. Am. Chem. Soc.* **2001**, *123*, 11341–11352.
(14) Ishima, R.; Torchia, D. *J. Biomol. NMR* **2003**, *25*, 243–248.
(15) Lundstrom, P.; Teilum, K.; Carstensen, T.; Bezsonova, I.; Wiesner, S.; Hansen, D. F.; Religa, T. L.; Akke, M.; Kay, L. E. *J. Biomol. NMR* **2007**, *38*, 199–212.
(16) Hansen, D. F.; Vallurupalli, P.; Lundstrom, P.; Neudecker, P.; Kay, L. E. *J. Am. Chem. Soc.* **2008**, *130*, 2667–2675.
(17) Ishima, R.; Baber, J.; Louis, J. M.; Torchia, D. A. *J. Biomol. NMR* **2004**, *29*, 187–198.
(18) Lundstrom, P.; Lin, H.; Kay, L. E. *J. Biomol. NMR* **2009**. In press.
(19) Skrynnikov, N. R.; Mulder, F. A. A.; Hon, B.; Dahlquist, F. W.; Kay, L. E. *J. Am. Chem. Soc.* **2001**, *123*, 4556–4566.
(20) Lundstrom, P.; Vallurupalli, P.; Religa, T. L.; Dahlquist, F. W.; Kay, L. E. *J. Biomol. NMR* **2007**, *38*, 79–88.
(21) Vallurupalli, P.; Hansen, D. F.; Stollar, E. J.; Meirovitch, E.; Kay, L. E. *Proc. Natl. Acad. Sci. U.S.A.* **2007**, *104*, 18473–18477.
(22) Igumenova, T. I.; Brath, U.; Akke, M.; Palmer, A. G. *J. Am. Chem. Soc.* **2007**, *129*, 13396–13397.
(23) Vallurupalli, P.; Hansen, D. F.; Kay, L. E. *J. Am. Chem. Soc.* **2008**, *130*, 2734–2735.
(24) Hansen, D. F.; Vallurupalli, P.; Kay, L. E. *J. Am. Chem. Soc.* **2008**, *130*, 8397–8405.
(25) Vallurupalli, P.; Hansen, D. F.; Kay, L. E. *Proc. Natl. Acad. Sci. U.S.A.* **2008**, *105*, 11766–11771.
(26) Gardner, K. H.; Rosen, M. K.; Kay, L. E. *Biochemistry* **1997**, *36*, 1389–1401.
(27) Tugarinov, V.; Kay, L. E. *ChemBioChem* **2005**, *6*, 1567–1577.
(28) Ottiger, M.; Delaglio, F.; Marquardt, J. L.; Tjandra, N.; Bax, A. *J. Magn. Reson.* **1998**, *134*, 365–369.
(29) Kontaxis, G.; Bax, A. *J. Biomol. NMR* **2001**, *20*, 77–82.
(30) Rath, A.; Davidson, A. R. *Protein Sci.* **2000**, *9*, 2457–2469.
(31) Drubin, D. G.; Mulholland, J.; Zhu, Z. M.; Botstein, D. *Nature* **1990**, *343*, 288–290.
(32) Lila, T.; Drubin, D. G. *Mol. Biol. Cell* **1997**, *8*, 367–385.
(33) Goto, N. K.; Gardner, K. H.; Mueller, G. A.; Willis, R. C.; Kay, L. E. *J. Biomol. NMR* **1999**, *13*, 369–374.
(34) Tugarinov, V.; Kay, L. E. *J. Biomol. NMR* **2004**, *28*, 165–172.
(35) Haynes, J.; Garcia, B.; Stollar, E. J.; Rath, A.; Andrews, B. J.; Davidson, A. R. *Genetics* **2007**, *176*, 193–208.
(36) Hansen, M. R.; Mueller, L.; Pardi, A. *Nat. Struct. Biol.* **1998**, *5*, 1065–1074.
(37) Delaglio, F.; Grzesiek, S.; Vuister, G. W.; Zhu, G.; Pfeifer, J.; Bax, A. *J. Biomol. NMR* **1995**, *6*, 277–293.
(38) Skrynnikov, N. R.; Dahlquist, F. W.; Kay, L. E. *J. Am. Chem. Soc.* **2002**, *124*, 12352–12360.
(39) Shaka, A. J.; Keeler, J.; Frenkiel, T.; Freeman, R. *J. Magn. Reson.* **1983**, *52*, 335–338.
(40) Marion, D.; Ikura, M.; Tschudin, R.; Bax, A. *J. Magn. Reson.* **1989**, *85*, 393–399.
(41) Morris, G. A.; Freeman, R. *J. Am. Chem. Soc.* **1979**, *101*, 760–762.
(42) Hansen, D. F.; Vallurupalli, P.; Kay, L. E. *J. Phys. Chem.* **2007**, PMID: 18001083.
(43) Markley, J. L.; Jorsley, W. J.; Klein, M. P. *J. Chem. Phys.* **1971**, *55*, 3604–3607.

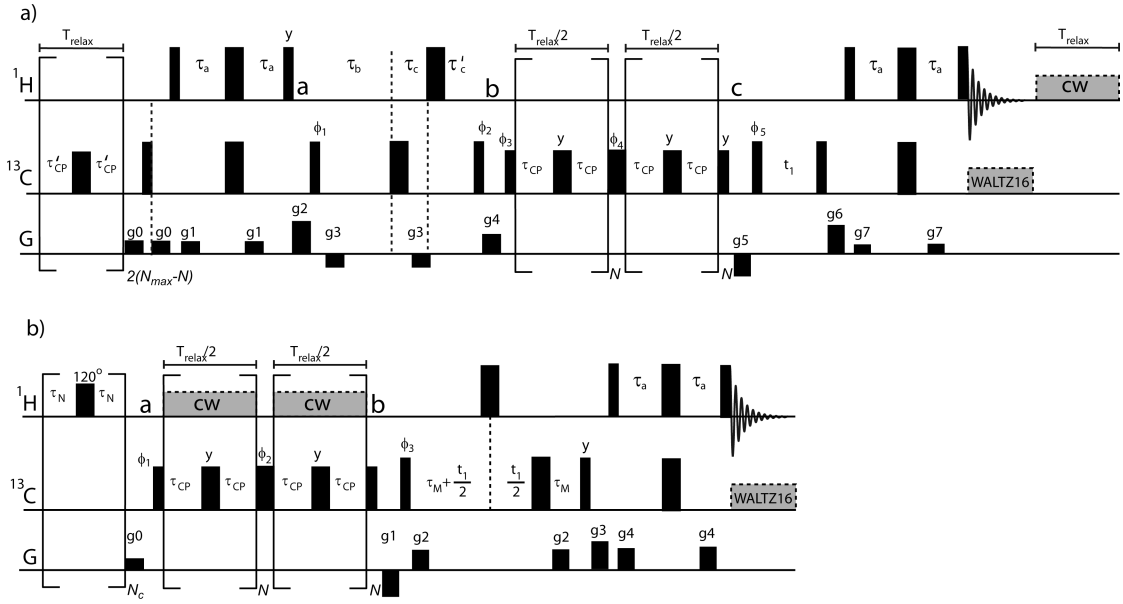

Figure 1. Pulse scheme for the measurement of methyl $^1H-^{13}C$ (a) spin-state selective and (b) CW relaxation dispersion profiles. ^1H and ^{13}C pulses that are shown with the highest vertical bars are applied at the highest power levels possible. ^{13}C pulses during the constant-time CPMG element, including the flanking 90° pulses are applied with a field strength of 16−17 kHz, with ^{13}C decoupling during acquisition achieved with a 2 kHz WALTZ-16 field.[39] The ^1H 180° pulse that is applied during the multiplet selection element between points *a* and *b* of scheme (a) is of the composite variety[29] $(90_x210_y90_x)$. All pulses are applied along the *x*-axis unless indicated otherwise. The durations τ_a and τ_b are set to <1/(4*J*) (1.8 ms) and 1/(4*J*) (2.0 ms), respectively, where *J* is the one-bond $^1H-^{13}C$ scalar coupling constant (∼125 Hz), $\tau_c = \tau_b - \Delta/2$ and $\tau'_c = \Delta/2$. *N* is any integer. Scheme (a): Delays $\tau_{eq} = 2-5$ ms were inserted immediately after gradients g4 and g5 to ensure that the relative amounts of magnetization of each state faithfully reports on equilibrium populations. In order to separate each multiplet component into a separate subspectra the approach of Kontaxis and Bax is employed[29] where four separate spectra, A−D, are acquired with the (ϕ_2,Δ) set to $(x,0)$, $(y,1/(6J))$, $(-x,1/(3J))$ and $(-y,1/(2J))$, respectively. These spectra are subsequently manipulated post acquisition to produce the linear combinations A+2B+2C+D, A+B−C−D, A−B−C+D, and A−2B+2C−D which result in subspectra containing the isolated $\beta\beta\beta$, $\alpha\beta\beta$, $\alpha\alpha\beta$, and $\alpha\alpha\alpha$ multiplets, respectively. The phase cycle is: $\phi_1 = 2(x,-x),2(-x,x)$, $\phi_3 = 2(x),2(-x)$, $\phi_4 = x,-x$, $\phi_5 = 2(x),2(-x)$, $\phi_{rec} = 2(x,-x),2(-x,x)$. Quadrature detection in F_1 is achieved via STATES-TPPI[40] of ϕ_5. Durations and strengths of the *z*-axis gradient pulses are (ms,G/cm), $g0 = (0.5,4)$, $g1 = (0.3,5)$, $g2 = (1.0,25)$, $g3 = (0.1,-4)$, $g4 = (1.5,6)$, $g5 = (1,-17)$, $g6 = (0.3,12)$, $g7 = (0.2,8)$. When $\tau_C > \tau'_C$ the second gradient *g*3 is applied as shown; otherwise, *g*3 is applied during the τ'_C duration. A ^1H CW field was applied for a duration T_{relax} immediately after acquisition to ensure the same degree of heating as in experiments recorded with scheme (b). Immediately prior to the first INEPT transfer[41] a ^{13}C CPMG element is applied, again to ensure uniform heating. N_{max} is the maximum value of *N* and $\tau'_{CP} = T_{relax}/(4(N_{max} - N))$. The ^1H carrier frequency is placed in the center of the methyl spectrum and then jumped to 4.7 ppm after gradient *g*6. Scheme (b): Many details are as for scheme (a) and are not repeated. The ^1H 180° pulse applied during the ^{13}C acquisition period is $(90_x180_y90_x)$.[29] Delays $\tau_{eq} = 2-5$ ms were inserted immediately after *g*1 and *g*3, $\tau_m = 770$ μs, $\tau_N = 2.5$ ms, $N_C = 400$. ^1H CW decoupling during the CPMG interval was achieved as described in the text and previously.[42] The carrier is placed at 4.7 ppm for the duration of the ^1H saturation period (composed of 120° pulses),[43] jumped to the methyl region of the spectrum and returned to 4.7 ppm after gradient *g*3. The phase cycle is: $\phi_1 = x,-x$, $\phi_2 = 4(x),4(-x)$, $\phi_3 = 2(x),2(-x)$, $\phi_{rec} = x,2(-x),x$. Quadrature detection in F_1 is achieved via STATES-TPPI[40] of ϕ_3. Durations and strengths of the *z*-axis gradient pulses are (ms,G/cm), $g0 = (1,5)$, $g1 = (0.5,-15)$, $g2 = (0.1,10)$, $g3 = (0.6,12)$, $g4 = (0.3,12)$. If $N = 0$, a ^1H CW decoupling field of duration T_{relax} is applied after acquisition to maintain a constant level of sample heating.

sets (Figure 1a) were recorded with acquisition times of (34 ms, 64 ms) in (t_1, t_2), 8 scans/FID, relaxation delay between scans of 2 s and 86 (800 MHz) or 64 (500 MHz) t_1 increments, for a total acquisition time of 0.93 h/2D spectrum at 800 MHz or 0.60 h at 500 MHz. Four spectra were recorded for each value of CPMG frequency to separate multiplet components into individual subspectra[29] (see below), leading to a net acquisition time of 86 (800 MHz) or 54 (500 MHz) hours for a complete data set. In the case of the CW dispersion experiments, recorded with the pulse scheme of Figure 1b, similar acquisition parameters to those listed above lead to net acquisition times of 16 and 20 h for complete data sets at 500 and 800 MHz (note that only one spectrum is required for each CPMG value in this case).

Dispersion data were processed and analyzed with the program NMRPipe,[37] and signal intensities were quantified by using the program FuDA (http://pound.med.utoronto.ca/software). Relaxation dispersion data were interpreted by using a two-state exchange model as described in the text and fitted using in-house software (http://pound.med.utoronto.ca/software) following protocols described in detail previously.[16,21,24] In cases where fits of dispersion profiles produced reduced χ^2 values >2, or where cross-peaks were highly overlapped, the data were excluded from further analysis. Dispersion profiles for all residues were analyzed together to extract global exchange parameters as well as residue-specific chemical shift and RDC differences between ground and excited states and intrinsic relaxation rates.

As described previously[21,24] and below, extraction of accurate RDC values for the excited state is predicated on determining the signs of ΔD, the differences in dipolar couplings between ground and excited states, which in turn depends on knowledge of the signs of the chemical shift differences, $\Delta\varpi_C$. For 9 of the 19 methyl groups in the Abp1p SH3 domain the signs of $\Delta\varpi_C$ could be obtained by a comparison of peak positions in HSQC/HMQC spectra recorded at 500 and 800 MHz following the method of Skrynnikov et al.[38] with the criterion that peak positions change by at least 1.5 ppb in the compared spectra in order to determine the sign. In the case of 8 of the 9 residues $|\Delta\varpi_C| \geq 0.1$ ppm, which has been chosen as a rough cutoff for which accurate signs could be obtained based on an analysis in a previous relaxation dispersion study.[16] In the case of Ile 26,δ1 $|\Delta\varpi_C| = 0.09$ ppm, however, the sign could be determined unequivocally since for this residue $|\Delta\varpi_H|$ is large (0.05 ppm) and the position of correlations in HMQC data sets in an exchanging system are sensitive to the value of $|\Delta\varpi_H|$.

RDC values for the apo Abp1p SH3 domain (visible, ground state) were measured using the scheme of Figure 1a with $T_{relax} = 0$, recorded on the 9% bound sample. Sums of the scalar and dipolar couplings were obtained from separation of multiplet components in each of four subspectra (see below). Experiments were repeated

Table 1. ^{13}C Frequencies of the Four Methyl Multiplet Components

multiplet[a]	s/n[b]	ν_C^{obsc}	$\Delta\nu_C^{obsd}$	corresponding density matrix element[e]
$\alpha\alpha\alpha$	3.8	$\nu_G - 3/2(J_G + D_G)$	$\Delta\nu_C - 3/2(\Delta J + \Delta D)$	$C_+\lvert\alpha\alpha\alpha\rangle\langle\alpha\alpha\alpha\rvert$
$\alpha\alpha\beta$	1	$\nu_G - 1/2(J_G + D_G)$	$\Delta\nu_C - 1/2(\Delta J + \Delta D)$	$C_+[\lvert\alpha\alpha\beta\rangle\langle\alpha\alpha\beta\rvert + \lvert\alpha\beta\alpha\rangle\langle\alpha\beta\alpha\rvert + \lvert\beta\alpha\alpha\rangle\langle\beta\alpha\alpha\rvert]$
$\alpha\beta\beta$	1	$\nu_G + 1/2(J_G + D_G)$	$\Delta\nu_C + 1/2(\Delta J + \Delta D)$	$C_+[\lvert\beta\beta\alpha\rangle\langle\beta\beta\alpha\rvert + \lvert\beta\alpha\beta\rangle\langle\beta\alpha\beta\rvert + \lvert\alpha\beta\beta\rangle\langle\alpha\beta\beta\rvert]$
$\beta\beta\beta$	3.8	$\nu_G + 3/2(J_G + D_G)$	$\Delta\nu_C + 3/2(\Delta J + \Delta D)$	$C_+\lvert\beta\beta\beta\rangle\langle\beta\beta\beta\rvert$

[a] Abbreviations for each multiplet component used in the text. [b] Relative *s*/*n* ratios in subspectra containing each of the multiplet components, neglecting relaxation. [c] Observed carbon frequency for each line of the ground state, where J_G and D_G are the scalar and dipolar couplings, respectively. [d] Effective chemical shift difference (Hz) that is extracted from fits of relaxation dispersion profiles for a methyl group undergoing two-site exchange in terms of $\Delta\nu_C = \nu_G - \nu_E$, $\Delta J = J_G - J_E$ and $\Delta D = D_G - D_E$. The difference in $\Delta\nu_C^{obs}$ between the two outer and the two inner lines is $3(\Delta J+\Delta D)$, and $(\Delta J + \Delta D)$ respectively. [e] Density matrix elements for each multiplet component, where $i,j,k \in \{\alpha,\beta\}$ in each wave function $\lvert ijk\rangle$ is the spin-state of one of the three methyl protons, H^i, H^j, H^k. C_+ in each of the expressions is given by $C_+ = C_X + iC_Y$, where C_j is the j component of ^{13}C magnetization.

in the absence of alignment to measure values of scalar couplings. Dipolar couplings for the holo-form of the protein were obtained in the same way as for the ground state of the apoprotein.

Spin-flip rates of methyl group protons, R_{1sel}, were quantified according to the relation $R_{1sel} = R_1(4C_ZH_ZH_Z) - R_1(2C_ZH_Z)$ where A_Z is the Z-magnetization of $A = {}^{13}$C or ^{1}H (ref 19). The relaxation rates of $4C_ZH_ZH_Z$ and $2C_ZH_Z$ were measured from a series of 2D ^{1}H$-^{13}$C data sets with parametrized relaxation delays varying from 5−150 ms using pulse sequences that are available upon request. $R_{1,sel}$ values less than 0.5 s^{-1} were obtained in all cases (25, 5 °C).

Results and Discussion

Measurement of Methyl ^{1}H$-^{13}$C RDCs in the Invisible Excited State. Prior to a description of the methodology developed for measuring methyl group RDC values that report on the invisible excited state it is useful to briefly mention a number of the basic experiments which have been developed to date for quantifying methyl group ^{1}H$-^{13}$C RDC values in "ground states" of proteins. Such a description places the work presented here in the proper context. In one experiment, proposed by Bax and co-workers, a series of 2D methyl ^{1}H$-^{13}$C correlation maps is recorded,[28] with each spectrum of the resultant 3D data set, $S(\omega^{13}C,t_2,\omega^1H)$, modulated by the evolution of ^{13}C magnetization from ^{1}H$-^{13}$C scalar and dipolar couplings that occurs during a separate time domain, t_2. Extraction of one-bond ^{1}H$-^{13}$C scalar couplings, J (unaligned samples), or the sum of scalar and dipolar couplings, $J+D$ (fractionally aligned samples), is readily accomplished by fitting the time-domain data to the appropriate function that accounts for the combined evolution of the four carbon multiplet components. A second class of experiment, developed by Kontaxis and Bax,[29] quantifies J or $J+D$ values, by measuring the separation between multiplet components in the ^{13}C frequency domain. In this approach a series of spectra are obtained that are manipulated postacquisition to generate four data sets, each of which contains one of the four possible methyl ^{13}C multiplet components that derives from magnetization evolution under the one-bond ^{1}H$-^{13}$C scalar and dipolar coupling interactions.

Clearly a prerequisite for the application of the methodology described above is that high resolution spectra be recorded that report directly on the conformer that is studied. This, of course, is possible for highly populated ground states of proteins but not in the context of invisible, excited conformers that is the focus of the study here. As described in detail previously,[21,22] the key in this case is to generate spin-state selective relaxation dispersion profiles that report on effective chemical shift differences between multiplet components in the ground (G) and excited (E) states ($\Delta\omega_C^{obs}$ in rad/s, $\Delta\varpi_C^{obs}$ in ppm or $\Delta\nu_C^{obs}$ in Hz) which in the case of molecular alignment depend on the differences in dipolar couplings between the states, $\Delta D = D_G - D_E$. Table 1 lists the resonance frequencies (in Hz) of each of the four multiplet components, ν_C^{obs}, the changes in frequencies, $\Delta\nu_C^{obs}$, that accompany an exchange event, as well as the corresponding density elements associated with each multiplet component.

Figure 1a shows the spin-state selective relaxation dispersion experiment that has been developed to measure methyl ^{1}H$-^{13}$C ΔD values in proteins. In the absence of the element between points a and b, in the limit that $T_{relax} = 0$ and neglecting pulse imperfections and relaxation, a 2D ^{1}H$-^{13}$C correlation map results with a 3:1:1:3 multiplet component ratio in F_1 that derives from ^{13}C magnetization coupled to all three methyl protons in the 'up' state (denoted by $\alpha\alpha\alpha$ and corresponding to the density matrix element $C_+\lvert\alpha\alpha\alpha\rangle\langle\alpha\alpha\alpha\rvert$, see Table 1), two 'up', one 'down' state ($\alpha\alpha\beta$), two 'down', one 'up' state ($\alpha\beta\beta$) and all 'down' state ($\beta\beta\beta$). The spacing between each of the lines is given to excellent approximation by J_G (unaligned sample) or $J_G + D_G$ (aligned). In principle, evolution during t_1 separates the components of magnetization according to spin-state so that by including a constant-time CPMG element between points b and c a series of dispersion profiles are generated that can be analyzed separately for each multiplet component to generate ΔD, as described briefly below and in more detail previously.[21,22,24]

In practice, however, the four lines generated for each methyl group can severely compromise resolution and we prefer, therefore to perform an experiment which isolates each multiplet component in a separate subspectrum, such that the number of resonances in each subspectrum is equal to the number in a decoupled spectrum. This isolation can be achieved using the approach of Kontaxis and Bax,[29] where the element between a and b of Figure 1a is used that allows antiphase ^{13}C magnetization, of the form $2C_YH_Z = 2C_Y(H_{1,Z} + H_{2,Z} + H_{3,Z})$, to evolve under scalar coupling (or $J_G + D_G$ in the case of weak alignment) for four different durations that generate differentially modulated spectra (see legend to Figure 1). Linear combinations of these data sets are generated, as described previously[29] and in the legend to Figure 1, to produce subspectra containing the isolated $\beta\beta\beta$, $\alpha\beta\beta$, $\alpha\alpha\beta$, and $\alpha\alpha\alpha$ multiplet components. The process of combining the data results in signal-to-noise (*s*/*n*) ratios in subspectra that differ from 3:1:1:3 that would otherwise be obtained if all components were in the same correlation map. In the absence of relaxation and omitting the CPMG element ($T_{relax} = 0$) the *s*/*n* ratio of subspectra containing the outer and inner multiplet components is $12/(10)^{1/2} \approx 3.8$, with the *s*/*n* of subspectra isolating the outer components approximately 35% of that generated from a standard HSQC experiment recorded in the same measuring time. There is a second reason beyond the issue of resolution that argues in favor of a scheme in which multiplet components are separated. Although care is taken to minimize the number of external proton spins by producing

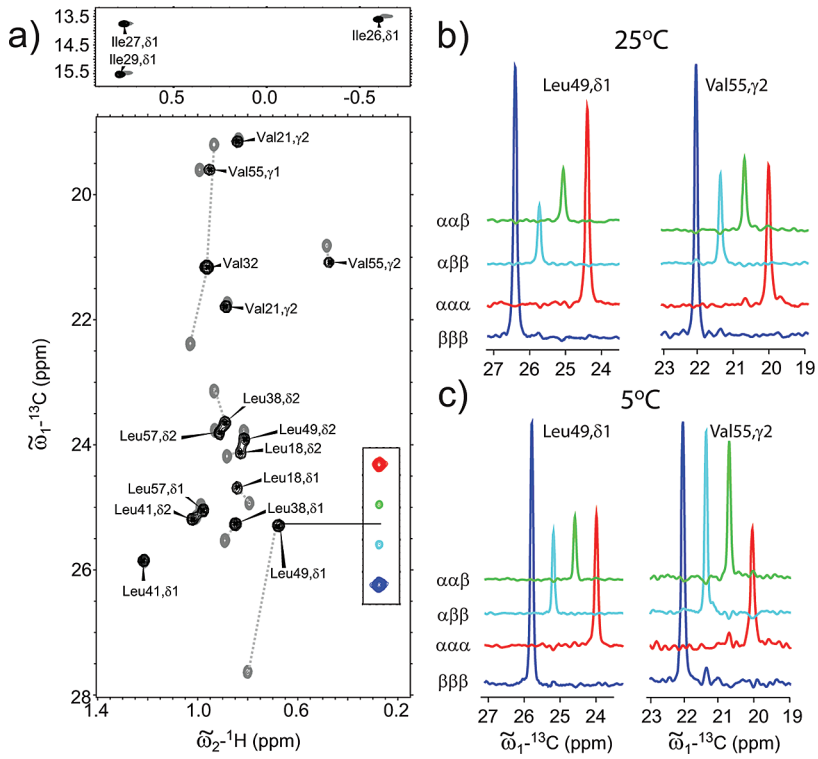

Figure 2. (a) $^{1}H-^{13}C$ HSQC spectra of the apo Abp1p SH3 domain (black) and holo-Abp1p SH3 domain bound to a peptide from the Ark1p protein (dark gray). Shifts in resonance positions that accompany peptide binding are indicated (gray dotted lines). Shown in the inset are four separate subspectra of Leu 49,δ1 (red, green, light-blue and dark-blue resonances correspond to the $\alpha\alpha\alpha$, $\alpha\alpha\beta$, $\alpha\beta\beta$ and $\beta\beta\beta$ of Table 1) acquired using the pulse sequence of Figure 1a ($\nu_{CPMG} = 1000\ s^{-1}$). (b,c) Traces at the ^{1}H resonance positions of Leu 49,δ1 and Val 55γ2 taken from subspectra that isolate each of the four multiplet components recorded with the scheme of Figure 1a, $\nu_{CPMG} = 1000\ s^{-1}$ under conditions of weak alignment (~50 mg/mL phage) at 25 °C (b) and 5 °C (c).

samples where protonation is confined to Ile, Leu and Val methyl groups (see below), 'residual' spin-flips during the CPMG element lead to exchange of multiplet components that can complicate extraction of robust exchange parameters as well as dipolar coupling values.[21,24] Intramultiplet cross-relaxation can be effectively suppressed by ensuring that magnetization associated with only one of the multiplet components is present at the start of the CPMG period, as was done recently for the measurement of excited state $^{1}HN-^{13}CO$ RDC values.[24] In fact, the dispersion profiles which are obtained with the scheme of Figure 1a where the spin-state selection element is placed prior to the CPMG pulse train, resulting in 'multiplet selective' subspectra, are equivalent to those which would be obtained in the case where only one of the four lines is present at the beginning of the CPMG element, so that excellent suppression of spin-flips is 'built into' the method.

Each spin-state selective dispersion profile depends on $\Delta\nu_C^{obs}$ which, in turn, is given by the appropriate linear combination of $\Delta\nu_C$ and ΔD (see Table 1). By contrast, ^{13}C dispersion experiments monitoring the decay of total carbon in-phase transverse magnetization during a CPMG pulse train depend on $\Delta\nu_C$ but not on ΔD and thus simultaneous fits of both spin-state selective and nonselective dispersion profiles in principle should provide a more robust approach for extraction of ΔD. Figure 1b illustrates the ^{13}C CW relaxation dispersion pulse scheme developed for quantifying $R_2^{eff}(\nu_{CPMG})$ of the total methyl carbon transverse magnetization. The experiment is very similar to one proposed by our group several years ago where magnetization originates on ^{13}C with sensitivity enhancement achieved through the development of the $^{1}H-^{13}C$ NOE.[19] However, in the present case ^{13}C magnetization is maintained as in-phase throughout the constant-time CPMG pulse train through the application of a ^{1}H continuous wave (CW) decoupling field, as has been described recently for the case of a CW ^{15}N CPMG experiment.[42] Here the ^{1}H CW field is applied at a strength, ν_{CW}, adjusted for each ν_{CPMG} value in such a way so as to ensure that an integral number of decoupling pulses is present in every τ_{CP} element ($2\tau_{CP}$ is the time between the centers of successive ^{13}C refocusing pulses). This is accomplished by choosing $\nu_{CW} = 2k\nu_{CPMG}$ where k is an integer, as described in detail previously.[42,44] Typically an average ^{1}H CW field of approximately 15−17 kHz is employed so that ν_{CW} varies by not more than ≈ 10% over the range of ν_{CPMG} values chosen. We have chosen to use a CW scheme rather than our previous experiment where scalar and dipolar coupled evolution proceed during each of the τ_{CP} periods that comprises the CPMG pulse train[19] because in the case where ^{1}H decoupling is applied, Figure 1b, the dispersions are completely independent of ΔD (ref 21) and the minimum ν_{CPMG} value that can be employed is half as large as would otherwise be possible.[42] This has significant advantages in cases where the exchange process is only a few hundreds/second, as in the example considered here.

In the case where a methyl group exchanges between a pair of conformations,

$$A \underset{k_{BA}}{\overset{k_{AB}}{\rightleftarrows}} B$$

the effective ^{13}C transverse relaxation rate that is measured by the CPMG pulse train of frequency $\nu_{CPMG} = N/T_{relax}$ (between points b and c of Figure 1a or a and b of Figure 1b) is given by $R_2^{eff}(\nu_{CPMG}) = R_{ex}(\nu_{CPMG}) + R_2^{\infty}$, where $R_{ex}(\nu_{CPMG})$ is the

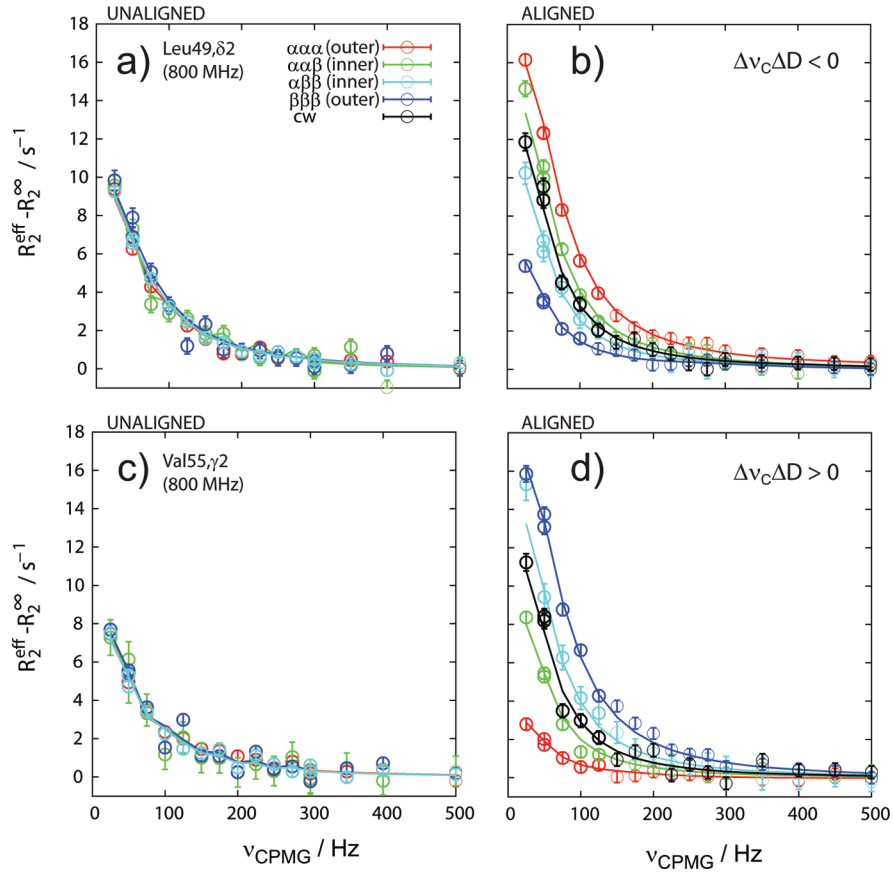

Figure 3. Spin-state selective and CW dispersion profiles, plotted as $R_{ex} = R_2^{eff} - R_2^{\infty}$, for Leu 49,$\delta$2 (a,b) and Val 55,$\gamma$2 (c,d) recorded on a sample of the Abp1p SH3 domain (9% Ark1p peptide), 25 °C, 800 MHz under conditions of no alignment (a,c) or weak alignment (b,d). Experimental data are shown by circles, with continuous lines corresponding to best fits to a global model of two-site chemical exchange (see text).

contribution due to chemical exchange and $R_2^{\infty} = R_2^{eff}(\nu_{CPMG}\rightarrow\infty)$. Experimentally $R_2^{eff}(\nu_{CPMG})$ can be determined from the relation $R_2^{eff}(\nu_{CPMG}) = (-1)/(T_{relax})\ \ln(I(\nu_{CPMG}))/(I(0))$, where $I(\nu_{CPMG})$ and $I(0)$ are the signal intensities in the presence and absence of the CPMG element,[45] respectively. By measuring $R_2^{eff}(\nu_{CPMG})$ as a function of ν_{CPMG}, $R_{ex}(\nu_{CPMG})$ is determined, and from simultaneous fits of both spin-state selective and nonselective dispersion data sets the parameters $\Delta\nu_C$, ΔD, $k_{ex} = k_{AB} + k_{BA}$ and p_B, the population of the excited state, can be derived[6,7] in much the same way as has been done previously to obtain backbone RDC values, except in that case only a pair of spin-state dispersion profiles were fit,[21,24] corresponding to $\Delta\nu^{obs} = \Delta\nu \pm \Delta D/2$. It is worth noting that the experimentally observed chemical shift differences, $\Delta\nu_C^{obs}$, obtained from fits of dispersion profiles derived from each multiplet component contain a contribution due to the change in $^1H-^{13}C$ scalar coupling between the ground and excited states of the molecule as well (see Table 1). However, in the case of a methyl group, the scalar coupling is relatively insensitive to structural changes and we have assumed $\Delta J = 0$ in what follows (average value of $|\Delta J| = 0.1$ Hz, based on studies of the system described below).

Test of the Methodology. As a test system to verify the methodology we have chosen a ligand binding reaction involving an SH3 domain from the yeast protein[30−32] Abp1p (P) and a 17-residue binding peptide from the protein Ark1p[35] (L) which exchange according to

$$P + L \underset{k_{off}}{\overset{k_{on}}{\rightleftarrows}} PL \qquad (1)$$

on a time-scale that is amenable to the CPMG relaxation dispersion technique.[21] When a small molar quantity of peptide is present in the sample ($[L] \ll K_D$), only the apo-Abp1p SH3 domain (ground state) will be observed directly in an NMR experiment. Values of ΔD and subsequently D_E can be obtained, however, using the experiments described above and can be subsequently cross-validated through comparison to directly measured values, obtained under conditions where enough peptide has been added to ensure that only the holo-Abp1p SH3 domain (PL) is present ($[L] \gg K_D$).

As described in Materials and Methods we have chosen a labeling scheme in which highly deuterated protein is prepared with $^{13}CH_3$ label confined to the δ1 position of Ile and to one of the two methyl groups of Val and Leu (the other methyl is $^{12}CD_3$).[34] This minimizes the number of protons in the sample and hence relaxation from external protons that leads to exchange between methyl multiplet components (spin-flips). Exchange between multiplet components 'averages out' differences in dipolar couplings between ground and excited states;[21] however, as is shown below, the effects of spin-flips are essentially negligible using this labeling scheme.

(44) Vallurupalli, P.; Scott, L.; Williamson, J. R.; Kay, L. E. *J Biomol NMR* **2007**, *38*, 41–46.
(45) Mulder, F. A. A.; Skrynnikov, N. R.; Hon, B.; Dahlquist, F. W.; Kay, L. E. *J. Am. Chem. Soc.* **2001**, *123*, 967–975.
(46) Werbelow, L. G.; Marshall, A. G. *J. Magn. Reson.* **1973**, *11*, 299–313.
(47) Kay, L. E.; Torchia, D. A. *J. Magn. Reson.* **1991**, *95*, 536–547.
(48) Tugarinov, V.; Scheurer, C.; Bruschweiler, R.; Kay, L. E. *J. Biomol. NMR* **2004**, *30*, 397–406.

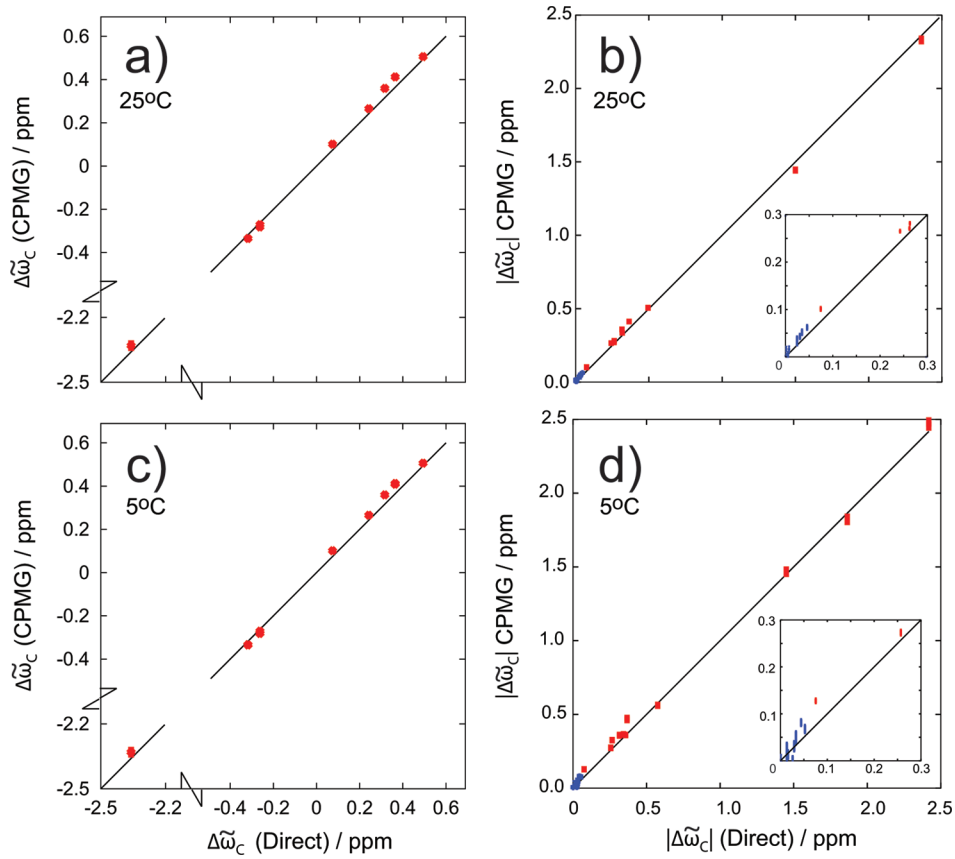

Figure 4. (a,c) Correlations of $\Delta\varpi_C$ values extracted from fits of CPMG dispersion data (Y-axis) with shift differences calculated directly from spectra of the apo and holo Abp1p SH3 domains (X-axis). CPMG data recorded using experiments of a and b of Figure 1 were fitted simultaneously (both 500 and 800 MHz data sets). Only data for which signs of $\Delta\varpi_C$ could be extracted are shown. (b,d) Correlations of $|\Delta\varpi_C|$ that include all (non-overlapped) residues for which robust fits of dispersion profiles were obtained, irrespective of whether the sign of the shift difference could be measured by the method of Skrynnikov (data in red)[38] or not (blue). Data recorded at 25 and 5 °C are shown in panels (a,b) and (c,d), respectively.

Initial methyl relaxation dispersion studies were recorded on an Abp1p SH3 domain sample with 9% mole fraction peptide using the pulse scheme of Figure 1b. Significant exchange contributions to R_2^{eff} were identified for many of the Ile, Leu and Val methyl groups in the protein located either at the binding interface (for example, Leu49, Val32, Leu38) or in the core of the domain (Leu18, Ile26, Val55) that undergo large changes in chemical shifts upon ligand binding, Figure 2a. Experiments using the pulse sequences described in parts a and b of Figure 1 were subsequently recorded under conditions of fractional alignment at temperatures of 25 and 5 °C where the rotational correlation times of the SH3 domain are approximately 5 and 10 ns, respectively. The four multiplet components generated by the spin-state selective sequence of Figure 1a were reasonably well isolated in all spectra b and c in Figures 2. The traces in Figure 2 were taken from spectra recorded with the highest pulsing rates ($\nu_{\text{CPMG}} = 1000$ s^{-1}, $T_{\text{relax}} = 40$ ms, 800 MHz) where magnetization transfer due to cross-relaxation between multiplet components is most effective. The two residues selected in b and c of Figure 2 produce the 'best' (Leu 49δ1) and among the 'worst' (Val 55γ2) levels of multiplet isolation. Note that the 'multiplet component selection element' (between points a and b of Figure 1a) works best for $D_G = 0$, but the efficient separation of components into their respective spectra even under conditions of alignment (largest D_G of 10.2 Hz in the present application) suggests that (i) this element is fairly robust, as described previously by Kontaxis and Bax,[29] and that (ii) the dipolar relaxation with external protons is small over the constant-time CPMG period employed for the measurements.

As described above, in the absence of relaxation the relative s/n of the individual multiplet-selective subspectra is expected to be in the ratio 3.8:1:1:3.8. Relaxation rates of the individual ^{13}C multiplet components can, however, be very different,[46] and in the limit of an isolated methyl group attached to a macromolecule and relaxing from ^{1}H$-^{13}$C dipolar interactions only, with very rapid methyl rotation, the relaxation rates of the outer lines are 9 times faster than those of the inner components.[47] Moreover, cross-correlation between dipolar and chemical shift anisotropy relaxation mechanisms contributes to an imbalance in the relaxation rates of the two outer or two inner lines[48] as is evident from traces in b and c of Figure 2. Notably, the average relative *s/n* ratios of subspectra comprising the fastest relaxing outer ($\alpha\alpha\alpha$) and inner ($\alpha\alpha\beta$) lines, V_{IO} (=outer/inner), is 3.8 ± 0.1 and 3.6 ± 0.2 for the Abp1p SH3 domain sample at 25 and 5 °C, respectively, measured with $T_{\text{relax}} = 0$ at 800 MHz. These ratios, based on peak volumes, are similar to the expected value of 3.8. By contrast, V_{IO} decreases to 2.6 ± 0.1(25 °C) and 1.7 ± 0.2(5 °C) for $T_{\text{relax}} = 40$ ms, $\nu_{\text{CPMG}} = 1000$ Hz, 800 MHz, reflecting the significant differential relaxation between multiplet components occurring during T_{relax} that increases as the molecular tumbling time gets larger. Indeed, it is even possible to have $V_{\text{IO}} < 1$ for residues with large methyl axis order parameters (rapid intrinsic transverse relaxation rates), such as is the case for Val 55γ2 (Figure 2c).

Figure 3 plots $R_{\text{ex}} = R_2^{\text{eff}} - R_2^{\infty}$ as a function of ν_{CPMG} for each of the four multiplet components of Leu 49,δ2 (a,b) and Val 55,γ2 (c,d) of the Abp1p SH3 domain (9% Ark1p peptide) quantified from spin-state selective data sets measured at 800

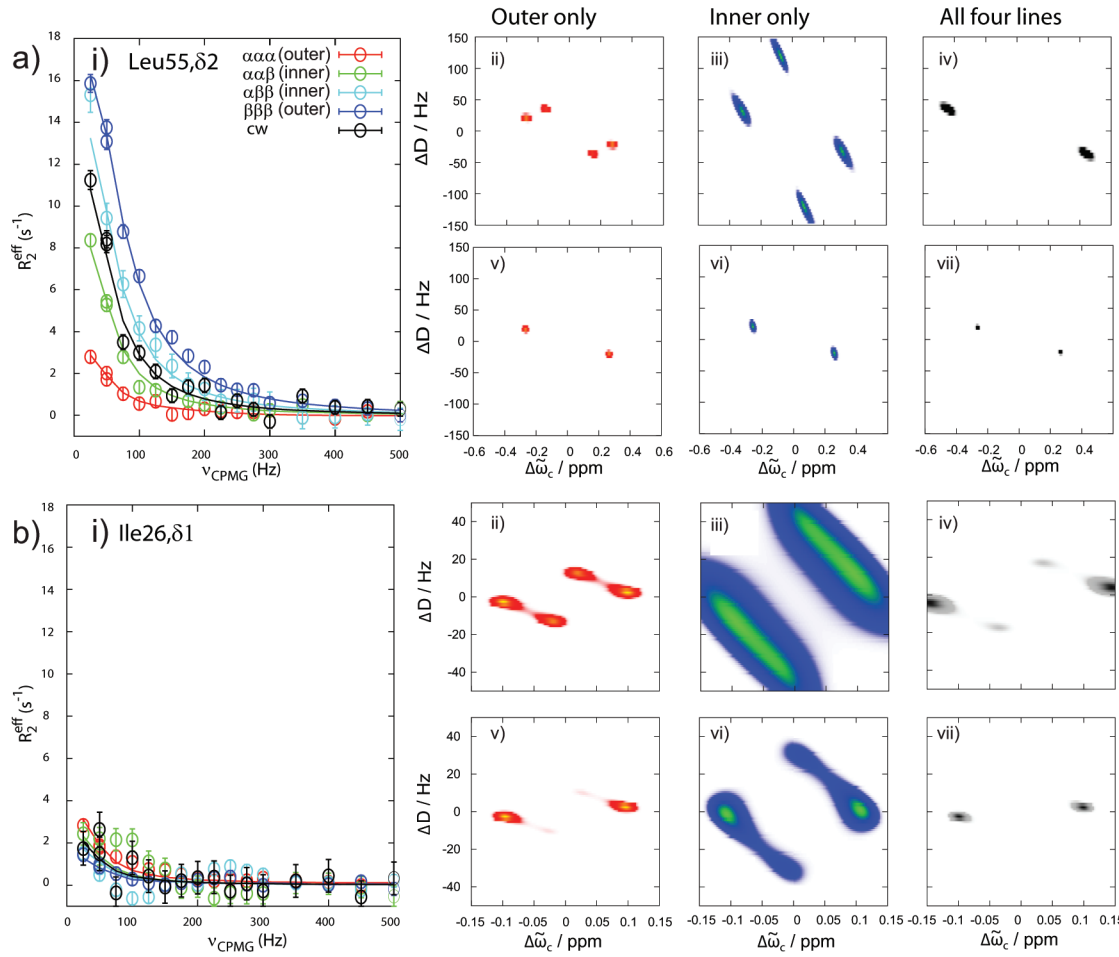

Figure 5. Spin-state selective and continuous wave (CW) dispersion data (i) acquired at 25 °C, 800 MHz and corresponding χ^2 probability surfaces for residues Leu55,δ2 (a) and Ile26,δ1 (b). Surfaces were calculated as $P(\Delta\varpi_C,\Delta D) = \exp(-(\chi^2 - \chi^2_{min})/2)$ where χ^2_{min} is the minimum of $\chi^2 = \sum_i[(R_i^{exp} - R_i^{calc}(\Delta\varpi_C,\Delta D))^2]/(\sigma_i^2)$, R_i^{exp} and R_i^{calc} are repectively experimental and calculated dispersion points, σ_i is the error in the experimental data. Values of $p_B = 10.8\%$ and $k_{ex} = 162$ s^{-1} (25 °C) determined from simultaneous fits of all data were used in the construction of the surfaces. Probability surfaces are calculated both using only spin-state selective data acquired at one field (800 MHz, ii, iii, iv) and using spin-state selective data recorded at 500 and 800 MHz in conjunction with CW data (500/800 MHz, v, vi, vii). In addition, the probability surfaces calculated from only the outer lines (ii, v), only the inner lines (iii, vi) and when using all four lines (iv, vii) are compared.

MHz. In the absence of alignment $\Delta D = 0$ and the variation of R_{ex} with ν_{CPMG} for each component is expected to be the same. Parts a and c of Figure 3 show that this is clearly the case. In contrast, upon alignment of the Abp1p SH3 domain, dispersion profiles generated for the individual multiplet components are not identical, Figures 3b,d, consistent with nonzero values of ΔD. The relative signs of $\Delta\nu_C$ and ΔD can be deduced through inspection of the $R_{ex}(\nu_{CPMG})$ profiles. In cases where $\Delta\nu_C\Delta D < 0$ the $R_{ex}(\nu_{CPMG})$ curve for the $\beta\beta\beta$ multiplet component lies below the corresponding profile for ααα, Figure 3b, since $\Delta\nu_C^{obs}(\beta\beta\beta) < \Delta\nu_C^{obs}(\alpha\alpha\alpha)$(see Table 1) with the opposite scenario occurring for $\Delta\nu_C\Delta D > 0$, Figure 3d.

Shown in Figure 4 are correlations of $\Delta\varpi_C$ values extracted from fits of dispersion profiles recorded at 25 °C (a,b) and 5 °C (c,d) with the corresponding values measured directly from apo and holo Abp1p SH3 domain samples. Shift differences from CPMG experiments were obtained from simultaneous fits of spin-state selective (Figure 1a) and CW (Figure 1b) dispersion profiles recorded at both 800 and 500 MHz (^{1}H frequencies), and it is clear that the accuracy of these values is high. As described in Materials and Methods the signs of CPMG-derived $\Delta\varpi_C$ values can be obtained in cases where $|\Delta\varpi_C| > 0.1$ ppm, and only those values for which signs are obtained are shown in a and c of Figure 4, while correlations for all extracted $|\Delta\varpi_C|$ values are indicated in b and d of Figure 4.

In general, obtaining accurate measures for ΔD is a more demanding task than for $\Delta\varpi_C$ since the latter can be measured from dispersion profiles that are not sensitive to ΔD, while spin-state selective relaxation rates, which are necessary for quantifying ΔD, depend on both $\Delta\varpi_C$ and ΔD (Table 1). Not surprisingly, therefore, more data are required for the extraction of accurate dipolar coupling values, and it is of interest to ask how much is really necessary. Consider first the case where dispersion profiles derived from the outer multiplet components only are fit and further that data from only a single static magnetic field are available. The $\beta\beta\beta$ and ααα profiles report on $|\Delta\nu_C^{obs}| = |\Delta\nu_C \pm 3/2\Delta D|$ and fits of these two dispersion curves produce four solutions (assuming perfect data), including $(\Delta\nu_{C,fit}, \Delta D_{fit}) = (\Delta\nu_C, \Delta D)$, $(-\Delta\nu_C, -\Delta D)$, $(3/2\Delta D, 2/3\Delta\nu_C)$, $(-3/2\Delta D, -2/3\Delta\nu_C)$. In a similar manner fitting only the inner lines $(|\Delta\nu_C^{obs}| = |\Delta\nu_C \pm 1/2\Delta D|)$ gives rise to the following solutions $(\Delta\nu_{C,fit}, \Delta D_{fit}) = (\Delta\nu_C, \Delta D)$, $(-\Delta\nu_C, -\Delta D)$, $(1/2\Delta D, 2\Delta\nu_C)$, $(-1/2\Delta D, -2\Delta\nu_C)$. It is clear that by fitting all four lines simultaneously the number of solutions is reduced by a factor of 2 to include only $(\Delta\nu_C, \Delta D)$, $(-\Delta\nu_C,-\Delta D)$. In principle, fits of any two spin-state selective profiles along with

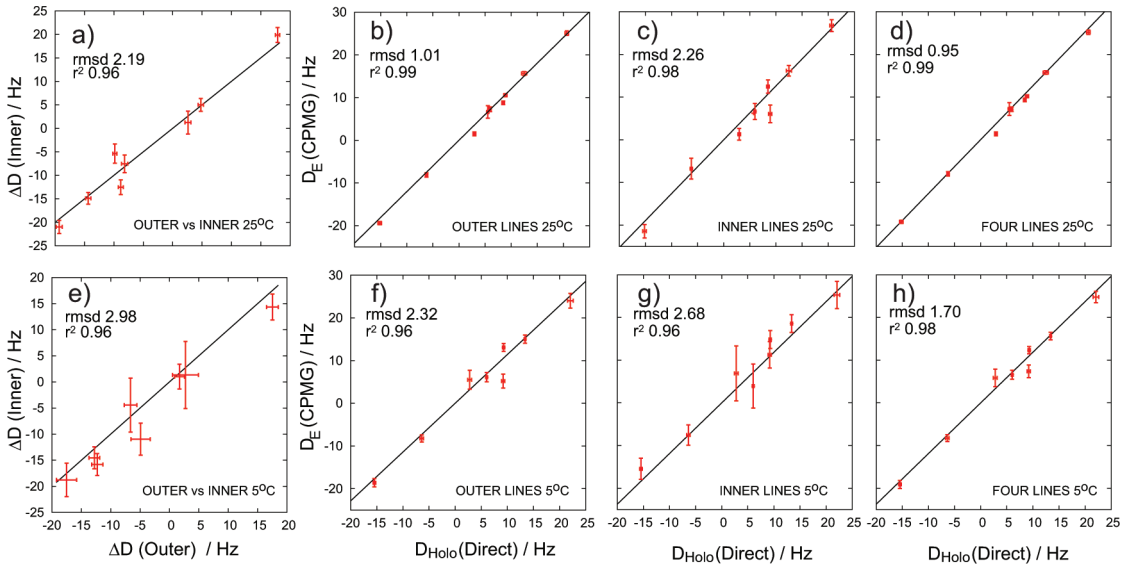

Figure 6. (a, e) Correlation between calculated ΔD values from analysis of CPMG relaxation data derived from the inner (Y-axis) and outer lines (X-axis). (b−d, f−h) Correlation between RDC values of the excited state corresponding to the Ark1p peptide bound form of the Abp1p SH3 domain, D_E, and RDC values measured directly of the fully bound SH3 domain, D_{Holo}, based on the analysis of two field (500 and 800 MHz) CPMG data containing only the outer multiplet components (b, f), only the inner components (c, g) and all four lines (d, h). In all cases CW dispersion profiles were included in the analysis. Residues shown are those for which the signs of $\Delta\omega_C$ and hence ΔD could be determined and where the reduced χ^2 of the data fit was less than 2. Results from data measured at both 25 °C (a−d) and 5 °C (e−h) are shown. Values of rmsd and r^2 (Pearson correlation coefficient) are shown for each panel, along with the best fit line, $y = mx$. The slopes differ from 1 in (b, c, d) and (f, g, h) since different amounts of alignment media were used for the CPMG and direct measurements (see Materials and Methods).

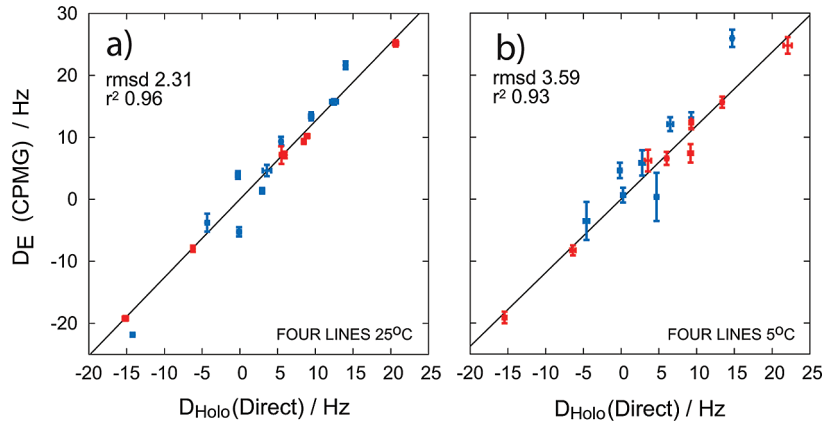

Figure 7. Correlation between RDC values of the excited state corresponding to the Ark1p peptide-bound form of the Abp1p SH3 domain, D_E, and RDC values measured directly of the fully bound SH3 domain, D_{Holo}, 25 °C (a) and 5 °C (b). All residues for which the reduced χ^2 values obtained in fits of CPMG data are less than 2 and for which well-resolved correlations are obtained in spectra are shown. In cases where signs of $\Delta\varpi_C$, and hence ΔD, could be determined by the method of Skrynnikov,[38] the points are in red; otherwise the sign of $\Delta\varpi_C$ was determined directly by inspection of spectra of the apo and holo SH3 domains and subsequently used to choose the correct sign for ΔD (points in blue).

CW dispersion data ($(|\Delta\nu_C^{obs}| = |\Delta\nu_C|)$ at a single field, or a pair of spin-state selective dispersion curves recorded at different static magnetic fields is sufficient in the absence of experimental error (in fact, less data may be sufficient); however, in our experience a combination of both spin-state selective and CW relaxation dispersion data sets recorded at a pair of static magnetic fields is much preferred. Note that it is not possible to choose from the two solutions $\{(\Delta\nu_C, \Delta D), (-\Delta\nu_C, -\Delta D)\}$ based on relaxation dispersion data alone, but once the sign of $\Delta\nu_C$ is available, then the correct solution can be selected.[21,24] Contours of fitted ΔD (Y-axis) vs fitted $\Delta\varpi_C$ (X-axis) values for Val55,δ2 and Ile26,δ1 (25 °C) reflecting the range of solutions from analysis of different quantities of dispersion data are shown in Figure 5. Panels ii−iv show results from fits of spin-state selective data recorded at a single field (800 MHz), where only outer (ii), inner (iii) or all four lines are considered (iv)), while panels (v−vii) display the results from fits where both spin-state selective and CW dispersion data recorded at 500 and 800 MHz are fit (outer only (v), inner only (vi), both outer and inner (vii)). It is particularly clear that, when dispersions are very small, the redundancy of data afforded by the multiple profiles is important. In the case of Ile26,δ1 (Figure 5b), for example, it is possible to extract an accurate excited state RDC value, despite the fact that dispersion profiles of no more than 2−3 s^{-1} are measured.

Figure 6 correlates dipolar coupling values which have been obtained from analysis of CPMG relaxation dispersion data sets with the corresponding values measured directly. In all cases CW dispersion data were included in the fitting process, with either the outer (b, f) or inner (c, g) or all four (d, h) of the multiplet selective profiles added as well. Data sets recorded at both 500 and 800 MHz were used in all fits. Parts a and e of

Figure 6 establish that reasonable correlations between ΔD values are obtained from fits of the two inner (Y-axis) or the two outer (X-axis) lines from the spin-state selective data. A comparison of ΔD values obtained from such independent fits provides an internal consistency check of the data. Values of $D_E = D_G - \Delta D$ can be readily calculated from ΔD values obtained from fits of relaxation dispersion profiles along with values of D_G of the populated, ground state that are measured directly. Parts b and c of Figure 6 show correlations between values of D_E generated from fits of the dispersion profiles based on analyses of the outer (b) and inner (c) lines from data sets recorded at 25 °C with the corresponding values, D_{Holo}, measured directly on the bound form of the SH3 domain; correlations from the 5 °C data are indicated in f and g of Figure 6. Better agreement is obtained when correlations involving the outer lines are compared relative to those focusing on the inner multiplet components (compare b and c or f with g) which reflects to a large extent the better s/n that is inherent in 'outer-line spectra' of small to moderately sized proteins and the fact that the outer lines are sensitive to $1.5\Delta D$ vs $0.5\Delta D$ for the inner components (Table 1). In this regard it is of interest to note that the rmsd values quantifying the level of agreement between D_E from CPMG and D_{Holo} from direct measurements based on fits of outer (b, f) and inner (c, g) lines are more similar for the measurements at lower temperature where the s/n of the outer-line and inner-line data sets become more comparable. Finally, D_E values are best estimated when all four spin-state selective dispersion profiles are fit (along with the CW data set), as indicated in d and h of Figure 6 where rmsd values of 0.95 and 1.7 Hz are obtained for the correlations of dipolar coupling values from data recorded at 25 and 5 °C, respectively. It is worth pointing out that all of the data have been analyzed neglecting the effects of contributions from protons proximal to the methyl group in question. When measured spin-flips are included in analyses of dispersion profiles of all four spin-state selective lines, the level of agreement with the RDC values obtained directly did not improve, consistent with the anticipated small effects from external proton spins.

The correlations in Figure 6 are those that include residues for which the sign of $\Delta\nu_C$ is available from peak positions in HSQC/HMQC data sets recorded at multiple fields.[19] Correlation plots, D_E (Y-axis) vs D_{Holo} (X-axis), composed of data from all residues that produce well-resolved correlations in spectra and for which small fitting errors are obtained (see Materials and Methods) are shown in a (25 °C) and and b (5 °C) of Figure 7. D_E values are based on analyses which include dispersion profiles from all four lines of the methyl multiplet as well as the CW data. In the case where the signs of $\Delta\nu_C$ could not be obtained experimentally ($\Delta\varpi_C < 0.1$ ppm[16]) they have been calculated from direct measurements and used to establish the correct D_E value (points in blue).

In summary, we have presented CPMG relaxation dispersion experiments for measuring methyl $^1H-^{13}C$ RDCs in invisible, excited states of proteins. The experiments complement previously developed methodology[21,23,24] which has focused on the measurement of backbone $^1HN-^{15}N$, $^1H^\alpha-^{13}C^\alpha$, and $^1HN-^{13}CO$ excited-state RDC values, as well as ^{13}CO RCSAs, by extending the approach to side-chain positions in proteins. Although the application in this study involves Ile, Leu, and Val methyl groups in highly deuterated proteins, it is possible to extend the number of probes to include Ala methyl groups since $^2H,^{13}CH_3-$Ala residues can be incorporated efficiently into highly deuterated proteins[49] as well as Met methyls which are often useful reporters[50] as well. It is anticipated that a combination of chemical shifts and anisotropic restraints will provide the basis for a detailed description of the structural features of excited states of proteins.

Acknowledgment. This work was supported by a grant from the Canadian Institutes of Health Research (CIHR) to L.E.K and by postdoctoral support in the form of fellowships to A.J.B. and D.F.H. from the European Molecular Biology Organization (EMBO) and the CIHR, respectively. We are grateful to Ms. Hong Lin for assistance with protein production. L.E.K. holds a Canada Research Chair in Biochemistry.

Supporting Information Available: One table with dipolar coupling and chemical shift values obtained from analysis of CPMG data along with the corresponding values generated from direct measurements; equations including the effects of spin-flips on the evolution of exchanging magnetization; complete author list for reference 11. This material is available free of charge via the Internet at http://pubs.acs.org.

JA903896P

(49) Isaacson, R. L.; Simpson, P. J.; Liu, M.; Cota, E.; Zhang, X.; Freemont, P.; Matthews, S. *J. Am. Chem. Soc.* **2007**, *129*, 15428–15429.
(50) Gelis, I.; Bonvin, A. M.; Keramisanou, D.; Koukaki, M.; Gouridis, G.; Karamanou, S.; Economou, A.; Kalodimos, C. G. *Cell* **2007**, *131*, 756–769.